

Local quantum criticality out of equilibrium - effective temperatures and scaling in the steady state regime

PEDRO RIBEIRO^{1,2}, QIMIAO SI³ and STEFAN KIRCHNER^{1,2}

¹ *Max Planck Institute for the Physics of Complex Systems - Nöthnitzer Str. 38, , D-01187 Dresden, Germany*

² *Max Planck Institute for Chemical Physics of Solids - Nöthnitzer Str. 40, D-01187 Dresden, Germany*

³ *Department of Physics and Astronomy, Rice University, Houston, Texas 77005, USA*

PACS 05.70.Jk – Critical phenomena in thermodynamics
 PACS 05.70.Ln – Thermodynamics, nonequilibrium
 PACS 72.10.Fk – Kondo effect, theory of electronic transport

Abstract – We study the out of equilibrium steady state properties of the Bose-Fermi-Kondo model, describing a local magnetic moment coupled to two ferromagnetic leads that support bosonic (magnons) and fermionic (Stoner continuum electrons) low energy excitations. This model describes the destruction of the Kondo effect as the coupling to the bosons is increased. Its phase diagram comprises three non-trivial fixed points. Using a dynamical large- N approach on the Keldysh contour, we study two different non-equilibrium setups: (a) a finite bias voltage and (b) a finite temperature gradient, imposed across the leads. The scaling behavior of the charge and energy currents is identified and characterized for all fixed points. We report the existence of a fixed-point-dependent effective temperature, defined though the fluctuation dissipation relations of the local spin-susceptibility in the scaling regime, which permits to recover the equilibrium behavior of both dynamical and static spin susceptibilities.

Introduction. – Understanding the physical properties of correlated systems away from thermal equilibrium has been a subject of intense research. The current interest in the theoretical description of far-from-equilibrium dynamics is partly driven by recent experimental achievements to probe non-thermal states in a controlled fashion [1–3]. Also, the ability to numerically address the time evolution of relatively large systems in conjunction with exact methods has lead to new insights, e.g. a better understanding of thermalization properties of interacting systems [4]. At present, it appears that the interplay between correlation effects and non-thermal boundary conditions can lead to a plethora of possible behaviors [4–6]. The existence of multiple steady-states selectively chosen by particular initial conditions [7] and of recurrent non-equilibrium solutions [8] are examples of such rich phenomena. Already classical systems away from equilibrium can show rich behaviors. A particularly interesting concept that emerged from the study of classical scale-free systems is the notion of effective temperatures based on local non-equilibrium fluctuation-dissipation relations [9,10]. In the context of scale-free quantum systems, the concept of effective temperatures has so far received only limited at-

tention [11–16]. Quantum critical systems, the quantum-analogs of classical scale-free systems, should be sensitive to any out-of-equilibrium drive, due to their gapless, scale-invariant spectrum. Unlike their classical counterparts, quantum critical systems link dynamical and static properties already at the equilibrium level. This raises the question if the concept of effective temperatures can be carried over to quantum scale-free systems in a meaningful way. While no such well-defined effective temperature was found in the ohmic spin-boson model [11], a preliminary study for a quantum critical system concluded that the notion of effective temperature based on an extension of the fluctuation-dissipation theorem can be meaningful [13]. For quantum critical systems possessing a gravity dual, it was recently suggested that an effective temperature characterizing the out-of-equilibrium current noise naturally emerges from the holographic mapping [15].

Studying the quantum relaxational ($\omega < T$) regime near quantum criticality faces methodological difficulties already at the equilibrium level and only few exactly solvable cases are available. Extending the study to non-thermal boundary conditions, poses further challenges.

In this letter, we address the out-of-equilibrium prop-

erties of current carrying steady states near Kondo-destroying quantum criticality in the spin-isotropic Bose-Fermi Kondo model (BFKM) [17–19] consisting of a quantum spin coupled to a fermionic and a sub-ohmic bosonic bath [20,21]. We address this model in terms of a dynamical large- N limit which gives access to the full quantum relaxational dynamics and treats equilibrium and out-of-equilibrium correlations on the same footing. This allows for a controlled comparison of the fluctuation-dissipation theorem with its out-of-equilibrium counterpart.

Model. – We consider the large- N version of the multi-channel BFKM (sketched in Fig.1-(a)) where the spin degree of freedom (\mathbf{S}) is generalized from $SU(2)$ to $SU(N)$ [20,22]. The fermionic excitations (c) of the bath transform under the fundamental representation of $SU(N) \times SU(M)$ with N the spin and M the charge channels. An out-of-equilibrium steady state is obtained by coupling the dot to two sets of such baths (*i.e.* leads) kept at different thermodynamic potentials [6]. The system is described by the Hamiltonian:

$$H = H_0 + H_I, \quad (1)$$

$$H_0 = \sum_{p,\alpha\sigma} \varepsilon_p c_{p\alpha\sigma}^\dagger c_{p\alpha\sigma} + \sum_{ql} w_q \Phi_{ql}^\dagger \cdot \Phi_{ql}, \quad (2)$$

$$H_I = \frac{1}{N} \sum_{\alpha, ll'} J_{ll'} \mathbf{S} \cdot \mathbf{s}_{\alpha ll'} + \frac{1}{\sqrt{N}} \sum_l g_l (\Phi_l^\dagger + \Phi_l) \cdot \mathbf{S}, \quad (3)$$

where σ and α are respectively the $SU(N)$ -spin and $SU(M)$ -channel indices, $l = L, R$ labels the left and right leads and p, q are momentum indices. The co-tunneling terms in Eq.(2) contain the local operators $s_{\alpha ll'}^i = \frac{1}{n_c} \sum_{pp'\sigma\sigma'} c_{p\sigma\alpha}^\dagger t_{\sigma\sigma'}^i c_{p'\sigma'\alpha l'}$ [23], with t the fundamental representation of $SU(N)$. In terms of their momentum counterparts, the local bosonic fields write as $\Phi_l^i = \frac{1}{\sqrt{n_\Phi}} \sum_q \Phi_{ql}^i$ (with $i = 1, \dots, N$). Here, n_c and n_Φ are the number of fermionic and bosonic single particle states taken to be proportional to the volume of the leads and set to infinity at the end of the calculation.

The impurity's $SU(N)$ -operators can be written, in terms of pseudo-fermions, $S^i = \sum_{\sigma\sigma'} f_\sigma^\dagger \tau_{\sigma\sigma'}^i f_{\sigma'}$, where i runs over the $N^2 - 1$ generators of $SU(N)$ and τ is an anti-symmetric representation of $SU(N)$ fixed by imposing the constraint $\hat{Q} = \sum_\sigma f_\sigma^\dagger f_\sigma = qN$ to the total number pseudo-fermions. In the path integral formalism, this constraint is enforced by a dynamical Lagrange multiplier λ .

Assuming that the exchange interaction derives from an Anderson-like impurity model [23] the matrix $J_{ll'}$ is given by $J_{ll'} = \sqrt{J_l J_{l'}}$ where $J_l \propto t_l^2/U$, with t_l the hopping term between the level and the leads and U the repulsive energy at the impurity site.

The spectral function of the bosonic bath is

$$\rho_\Phi(\omega) = \frac{1}{n_\Phi} \sum_q \delta(\omega - w_q) \propto \omega^{\alpha_\Phi - 1}, \quad (4)$$

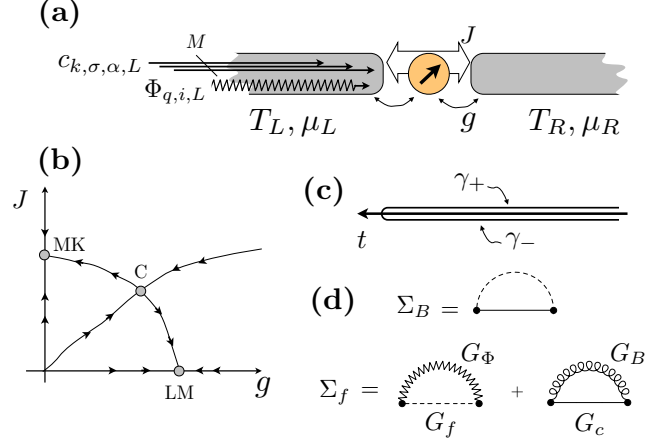


Fig. 1: (a) A sketch of the non-equilibrium setup of the BFKM model. (b) The phase diagram of the BFKM model encompassing three fixed points: multichannel Kondo (MK), critical (C) and local moment (LM). The parameters J and g are the couplings of the local moment to the fermions and bosons, respectively. The arrows denote the RG flow to the three fixed points, over-screened Kondo, LM and critical. (c) Sketch of the Keldysh contour $\gamma = \gamma_+ + \gamma_-$. (d) Large- N self-energy diagrams corresponding to Eqs. (5,6).

for $|\omega| < \Lambda$, where Λ is some cut-off scale. The fermionic bath is characterized by a constant density of states at the Fermi level $\rho_c(\omega = 0)$ that for $g = 0$ yields to the Kondo energy scale $T_K = \rho_c(0)^{-1} e^{-\frac{1}{(J_L + J_R)\rho_c(0)}}$.

The phase space of this model encompasses three fixed points, located in the $T = 0, V = 0$ hyperplane, that can be accessed by varying the ratio g/J , see Fig.1-(b). An over-screened multichannel Kondo phase (MK) at small g/J is separated from a local moment (LM) phase by an unstable critical point (C). The characterization of each phase and the scaling laws for the different quantities were obtained in [19,20] both by perturbative RG and large- N methods.

We consider a non-equilibrium setup where the two leads, initially decoupled from the impurity (for $t < t_0$), are held at chemical potentials $\mu_L = -\mu_R = |e|V/2$ and at temperatures T_L and T_R . As the leads are considered to be infinite reservoirs, its bosonic and fermionic distributions functions are given respectively by $n_{b,l}(\omega) = \frac{1}{e^{\beta_l \omega} - 1}$ and $n_{f,l}(\omega) = \frac{1}{e^{\beta_l(\omega - \mu_l)} + 1}$ with $\beta_l = T_l^{-1}$. At $t = t_0$ the coupling between the leads and the impurity (H_I) is turned on. We address the steady state regime by formally setting $t_0 \rightarrow -\infty$.

Dynamical large- N out-of-equilibrium. We follow the dynamic large- N approach of Ref. [20], generalized to an out-of-equilibrium setup in Ref. [6]. The generating function writes $Z = \int Dc Dc^* D\Phi D\Phi^* Df Df^* D\lambda e^{-S}$, with S the action associated with Eq.(2) and where the integration of the fields is performed over the forward (γ_+) and backward (γ_-) Keldysh branches (see Fig.1-(c)). Our approach generalizes the calculations under the equilibrium

conditions [20, 22] to the Keldysh contour¹ [24].

In the steady-state regime $G_a(t, t') = G_a(t - t')$ (with $a = f, B$) and the Keldysh equation $G_a^{>, <} = G_a^R \Sigma_a^{>, <} G_a^A$ holds for the local pseudo-particle Green's functions. The saddle-point equations simplify to

$$\Sigma_B^{>, <}(t) = iG_f^{>, <}(t) G_c^{<, >}(-t) \quad (5)$$

$$\Sigma_f^{>, <}(t) = -i\kappa G_B^{>, <}(t) G_c^{<, >}(t) + ig^2 G_f^{>, <}(t) [G_\Phi^{>, <}(t) + G_\Phi^{<, >}(-t)] \quad (6)$$

$$-iG_f^{<}(t) = q, \quad (7)$$

where $q = \frac{Q}{N}$, $\kappa = \frac{M}{N}$, $g^2 = \bar{g}_L g_L + \bar{g}_R g_R$, and $J = J_L + J_R$.

The local quantities $G_c(t) = \frac{1}{n_c} \sum_p \frac{1}{J} [J_L G_{c,pL}(t) + J_R G_{c,pR}(t)]$ and $G_\Phi(t) = \frac{1}{n_\Phi} \sum_q \frac{1}{q^2} [\bar{g}_L g_L G_{\Phi qL}(t) + \bar{g}_R g_R G_{\Phi qR}(t)]$ are defined in terms of the lead's fermionic and bosonic Green's functions and the Green's functions of the local fields are given by $G_f^{-1}(t) = -(\partial_t - \mu) - \Sigma_f(t)$ and $G_B^{-1}(t) = J^{-1} - \Sigma_B(t)$, with $-i\mu$ the saddle point value of the Lagrange multiplier field λ .

For the numerical evaluation of the saddle point equations, we use $\rho_c(\omega) = \frac{1}{\pi D} e^{\frac{1}{\pi}(\frac{\omega}{D})^2}$, $\rho_\Phi(\omega) = \Theta(\omega) \frac{2}{\Lambda \Gamma(\frac{\alpha_\Phi}{2})} (\frac{\omega}{\Lambda})^{\alpha_\Phi - 1} e^{-(\frac{\omega}{\Lambda})^2}$, where D is a high energy cutoff of the fermionic density of states, $\Lambda = 0.1 D$, $\kappa = 1/2$ and $q = 1/2$.² For definiteness we also take $\alpha_\Phi = 5/4$.

The self-consistent equations were solved iteratively on a logarithmic discretized grid with $\simeq 250$ points ranging from $-10D$ to $10D$. The criterium for convergence was that the relative difference of two consecutive iterations was less than 10^{-6} . We also set $J\rho_c(0) = 0.8/\pi$, yielding a critical value of the bosonic coupling of $g_c \simeq 0.2199J$. We checked that our results hold for other choices of parameters.

The scaling properties of the model at equilibrium are analyzed in Ref. [19, 20]. The scaling exponents of the auxiliary Green functions G_f and G_B are summarized in table 1, where α_f and α_B are defined through

$$G_a(\omega, T) = |\omega|^{1-\alpha_a} \Psi_a(\omega/T) \quad (a = f, B), \quad (8)$$

and $\Psi(x)$ is a smooth scaling function with $\Psi(0) \neq 0$.

The imaginary part of the spin susceptibility behaves as

$$\chi''(\omega) \propto \text{sgn}(\omega) |\omega|^{\alpha_\chi}, \quad (9)$$

where $\alpha_\chi = 2\alpha_f - 1$.

¹The $SU(M)$ symmetry of the model ensures that the propagator of the local bosonic field B is independent of the channel index α . The singular nature of the matrix $J_{ll'}$ substantially simplifies the treatment as the combination $\sqrt{J_R/J_{BL}} - \sqrt{J_L/J_{BR}}$ decouples from the equations and one is left with a single scalar field $B = \sqrt{J_L/J_{BL}} + \sqrt{J_R/J_{BR}}$.

² $q = 1/2$ corresponds to a particle-hole symmetric setup. Note, the out-of-equilibrium conditions considered here respect particle-hole symmetry.

	MK	C	LM
α_f	$\frac{1}{1+\kappa}$	$2 - \frac{1}{2}\alpha_\Phi$	$2 - \frac{1}{2}\alpha_\Phi$
α_B	$1 - \frac{1}{1+\kappa}$	$\frac{1}{2}\alpha_\Phi$	$1 - \frac{1}{2}\alpha_\Phi$

Table 1: Scaling exponents of the auxiliary Green functions G_f and G_B here evaluated for $\kappa = 1/2$ and $\alpha_\Phi = 5/4$.

We report results for two out-of equilibrium situations: (a) a finite bias voltage applied across the leads $\mu_L = -\mu_R = V/2$ kept at the same temperature T and (b) a finite temperature gradient $\Delta T = T_L - T_R$ with $\mu_L = \mu_R = 0$.

Observables. The particle number and energy currents, denoted respectively \mathcal{J}_n and \mathcal{J}_e , obtained from the continuity equation, are $\mathcal{J}_{b,a,l} = -\partial_t \langle \mathcal{Q}_{b,a,l}(t) \rangle$, where $b = n, e$ (for particle and energy current respectively), $a = c, \Phi$ (for the fermionic and bosonic fields), $\mathcal{Q}_{n,a,l} = N_{a,l}$ is the number of particles a on the lead l and $\mathcal{Q}_{e,a,l}$ is the part of the Hamiltonian of the particles a restricted to the lead l . Explicitly, one gets

$$\mathcal{J}_{b,\Phi,l} = -i \frac{1}{\sqrt{N} n_\Phi} \sum_{i\sigma\sigma';q} j_{b,\Phi,q} [g_l \tau_{\sigma\sigma'}^i \langle f_\sigma^\dagger f_{\sigma'} \Phi_{qil} \rangle - \text{c.c.}], \quad (10)$$

$$\mathcal{J}_{b,c,l} = -i \frac{1}{N n_c} \sum_{\alpha\sigma\sigma';kp} j_{b,c,p} \left\{ J_{l'l} \left[\langle f_{\sigma'}^\dagger f_\sigma c_{k\alpha\sigma'l}^\dagger c_{p\alpha\sigma'l} \rangle - \frac{1}{N} \langle f_{\sigma'}^\dagger f_{\sigma'} c_{k\alpha\sigma'l}^\dagger c_{p\alpha\sigma'l} \rangle - \text{c.c.} \right] \right\} \quad (11)$$

where $l' \neq l$, $j_{n,\Phi,q} = j_{n,c,p} = 1$, $j_{e,\Phi,q} = w_q$, and $j_{n,c,p} = \varepsilon_p$. All operators inside brackets are computed at equal time. Note that for the fermions the identity $\mathcal{J}_{b,c,L} = -\mathcal{J}_{b,c,R}$ immediately follows. This does not hold for the bosons as their number is not conserved by the Hamiltonian. In terms of the particle current, the total electric current leaving the left lead is given by $I = -|e| \mathcal{J}_{n,c,L}$, where $|e|$ is the absolute value of the electron charge.

The correlation functions appearing in Eqs.(10,11) involve impurity as well as bath degrees of freedom. As Wick's theorem no longer holds, the approach taken here consists in inserting external sources, conjugate to the c, Φ and f fields, that respect the Keldysh structure. By varying the action with respect to the sources one obtains the desired correlation functions. The computation of the explicit form of generic observables in terms of the distribution functions of the local and bath fields turns out to be rather involved. This cumbersome approach is necessary as T -matrix-based arguments are not ensured to hold for the large- N generalization of the BFKM. Interestingly our results are qualitatively compatible with the T -matrix based derivations [6, 20] whenever a comparison is possible.

Effective temperature. The steady-state fluctuation dissipation ratio (FDR) is defined, for dynamical observable $O(t, t') = O(t - t')$, as $\text{FDR}_O(\omega) = \frac{[O^>(\omega) + O^<(\omega)]}{[O^>(\omega) - O^<(\omega)]}$,

with $O^{>/<}(\omega)$ being the Fourier-transforms of the greater/lesser components: $O^{>/<}(t, t')$ for $t \in \gamma_{-/+}$ and $t' \in \gamma_{+/-}$ (the definition of the Keldysh branches γ_{\pm} is given in Fig.1-c). At equilibrium, the fluctuation dissipation theorem fixes $\text{FDR}_O(\omega) = \text{FDR}_{\text{Eq}}(\omega) = \tanh(\beta\omega/2)^{-\zeta}$ (with $\zeta = \pm 1$ for bosonic or fermionic operators) uniquely. For a generic out-of-equilibrium system, the functional form of the FDR differs from the equilibrium one.

An observable and frequency dependent “effective temperature”, $\beta_{\text{eff},O}(\omega)$, can be defined by requiring that $\tanh(\beta_{\text{eff},O}(\omega)\omega/2)^{-\zeta} = \text{FDR}_O(\omega)$ [13, 25]. For the regimes where the out-of-equilibrium drive is much smaller than the temperature, linear response theory can be used and the equilibrium functional form is expected to hold. Here we follow Refs. [9, 11] and define an effective temperature for the observable O by its asymptotic low frequency behavior

$$\beta_{\text{eff},O} = \beta_{\text{eff},O}(0) = \lim_{\omega \rightarrow 0} \frac{\text{FDR}_O(\omega)^{-\zeta}}{\omega/2}. \quad (12)$$

As shown below the effective temperature defined in this way holds for all frequencies in the scaling regime. From this expression, one obtains an observable-dependent effective temperature. Here we will consider, $T_{\text{eff},\chi}$, $T_{\text{eff},B}$ and $T_{\text{eff},f}$, computed from Eq.(12) using the pseudo-particle Green’s functions and the impurity susceptibility. A preliminary study of the spin susceptibility near the quantum critical LM regime indicated that an effective temperature can be defined in the corresponding scaling regime [13]. In this letter, we demonstrate that the notion of effective temperature can be successfully used whenever the system displays critical scaling in the nonequilibrium regime. The evaluation of the pseudo-particle quantities has two purposes: (i) First, the agreement between these quantities indicates that it is possible to define an observable independent effective temperature. (ii) Secondly, as Wick’s theorem applies to higher spin correlators in the large- N limit, such observables will automatically have the same effective temperature T_{eff} .

Results . –

(a) *Finite bias voltage.* Fig.2 shows the behavior of the spin-susceptibility of the impurity and the effective temperatures at the MK ($g = 0$), C ($g = g_c$) and LM ($g = 2.5g_c$) fixed points for $V \neq 0$ and $\Delta T = 0$.

The effective temperatures (Eq.(12)), given in Fig.2-(right panel), are obtained for $T = 5 \times 10^{-8}T_K$ by varying V alone. The full scaling form of $T_{\text{eff},\chi}$ is given in the inset. A clear linear regime can be observed for small V where the effective temperatures approach the temperature of the leads $T_{\text{eff},\chi/f/B}/T \simeq 1$. As V/T increases and the non-linear regime sets in, differences between the different fixed points are observed. In the Kondo and critical cases, all the effective temperatures increase with V/T . In the LM fixed point the linear regime where $T_{\text{eff},f/\chi} \simeq T$ extends to much larger values of V . This can be intuitively

understood by the fact that, in this case, the impurity spin is mainly interacting with the bosonic bath which is insensitive to the chemical potential drop.

A somehow surprising result is the fact that by replacing T by $T_{\text{eff},\chi}$ the equilibrium universal scaling form of the spin-susceptibility is recovered for all cases. Fig. 2-left panel shows that the imaginary part of the susceptibility as a function of frequency follows the same equilibrium scaling form with T substituted by $T_{\text{eff},\chi}$. The static susceptibility as a function of $T_{\text{eff},\chi}$ (middle panel) also follows the same equilibrium universal curve.

This suggests that $T_{\text{eff},\chi}$ is a useful concept to interpret the dynamic and static susceptibility out of equilibrium, even in the non-linear regime where a single effective temperature could not be defined.

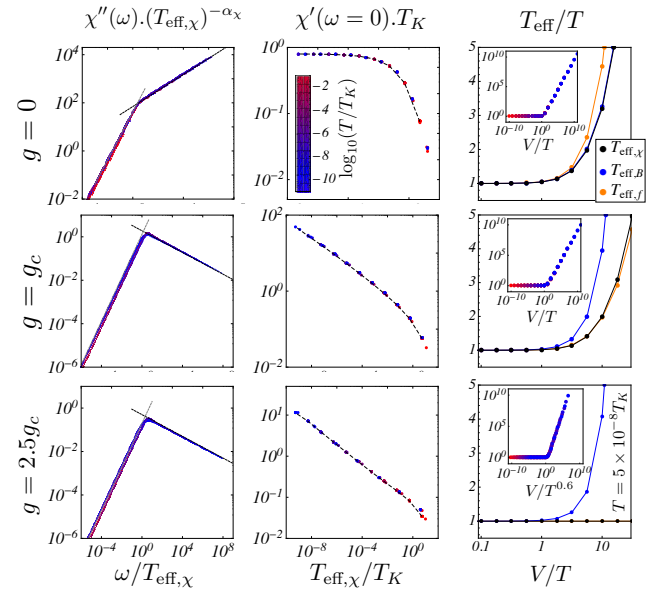


Fig. 2: Left panel - Imaginary part of the spin-susceptibility $\chi''(\omega)$ as a function of frequency rescaled by $T_{\text{eff},\chi}$ computed for the Kondo ($g = 0$), the critical ($g = g_c$) and the LM ($g = 2.5g_c$) fixed points for different temperatures and bias voltages. The colored points are numerical results obtained for different temperatures (see inset caption) and the dashed black lines are fits to the equilibrium form. Middle panel - Static spin-susceptibility $\chi'(\omega = 0)$ as a function of $T_{\text{eff},\chi}$. Points with the same color are computed for the same values of T and different values of $V \neq 0$. The black lines display the equilibrium result. For both quantities $\chi''(\omega)$ and $\chi'(\omega = 0)$, the equilibrium scaling form holds by replacing T by $T_{\text{eff},\chi}$. Right Panel - Comparison between the different effective temperatures, computed by Eq.(12), as a function of V/T for a fixed T . The inset shows the scaling collapse of $T_{\text{eff},\chi}/T$ for different values of T and V .

I-V Characteristics. We now turn to the discussion of the IV characteristics, see Fig. 3. For $V \rightarrow 0$ the conductance increases for low temperatures and approaches a constant, G_0 at zero temperature. Fig. 3 shows the behavior of the current for the three regimes for a non-equilibrium setup with $\Delta T = 0$, $V \neq 0$, computed at

different temperatures. Here we define the linear conductance per channel as

$$G(T) = \frac{1}{M} \left. \frac{d\mathcal{J}_n}{dV} \right|_{V=0}.$$

For $g = 0$ the current is proportional to the applied voltage $\mathcal{J}_n \simeq G_0 V$ as long as $V, T \ll T_K$. Outside of the scaling regime, i.e. for $V, T > T_K$, \mathcal{J}_n/V drops rapidly when V or T increase. For $0 < g < g_c$, \mathcal{J}_n/V still approaches G_0 for small voltages, however the drop in the conductance arises for a smaller energy scale $V, T \simeq T_K^*(g)$ where $T_K^*(g = 0) = T_K$ and $T_K^*(g = g_c) = 0$.

In the LM regime the $T = 0$ conductance vanishes as the impurity effectively decouples from the conduction electrons. The dependence of the current as $T, V \rightarrow 0$, in the linear and non-linear response regimes develop different power law behaviors. The exponents are well fitted by the scaling ansatz of Ref. [6]: in the linear response regime $\mathcal{J}_n \propto T^{4-\alpha_\Phi} V$ and in the non-linear case $\mathcal{J}_n \propto V^{3-\alpha_\Phi}$.

In the critical regime ($g = g_c$) the relation between the current and the applied voltage is still linear ($\mathcal{J}_n = G_c V$) as first found in [6], however the typical values of the critical conductance G_c are much smaller than G_0 . The linear and nonlinear regimes are characterized by slightly different values of the conductance separated by a crossover. In Ref. [6] a similar behavior was reported but a larger variation between the linear and non-linear conductance was found. This can be explained by the fact that Ref. [6] considers the current computed using the T-matrix from the underlying Anderson model.

(b) *Finite temperature gradient.* Fig.4 shows the dependence of χ and T_{eff} on the out-of-equilibrium drive parametrized by $\Delta T/\bar{T}$ where $\bar{T} = (T_L + T_R)/2$ is the average temperature. In this case, for all the critical points, the effective temperatures are strongly affected by changes in $\Delta T/\bar{T}$, since fermionic and bosonic excitations are susceptible to a gradient in T across the impurity. The agreement between the effective temperatures computed for the three different quantities is much better than in case (a) (where $\Delta T = 0, V \neq 0$).

As for the setup (a), χ as a function of $T_{eff,\chi}$, is found to follow the equilibrium scaling form for all regimes. The fact that T_{eff} is now strongly renormalized at all fixed points shows that the scaling behavior is robust.

Thermal transport. Due to the particle-hole symmetry, ΔT across the leads does not induce a net particle current but there is an energy flow from the hot to the cold lead. We consider the fermionic contribution to this energy flow, defined in Eq.(11) As the bosonic contribution to the energy current turns out to be vanishingly small, we focus on the fermionic part of the energy flow.

Fig. 5 shows the scaling form of the energy current $\mathcal{J}_e = \mathcal{J}_{e,c,L}$ as a function of $\Delta T/\bar{T}$ for the different regimes. In the Kondo regime, for $g = 0$, \mathcal{J}_e/\bar{T} scales linearly with $\Delta T/\bar{T}$ as long as $\bar{T} \lesssim T_K$. For $\bar{T} \gg T_K$, \mathcal{J}_e/\bar{T} drops to

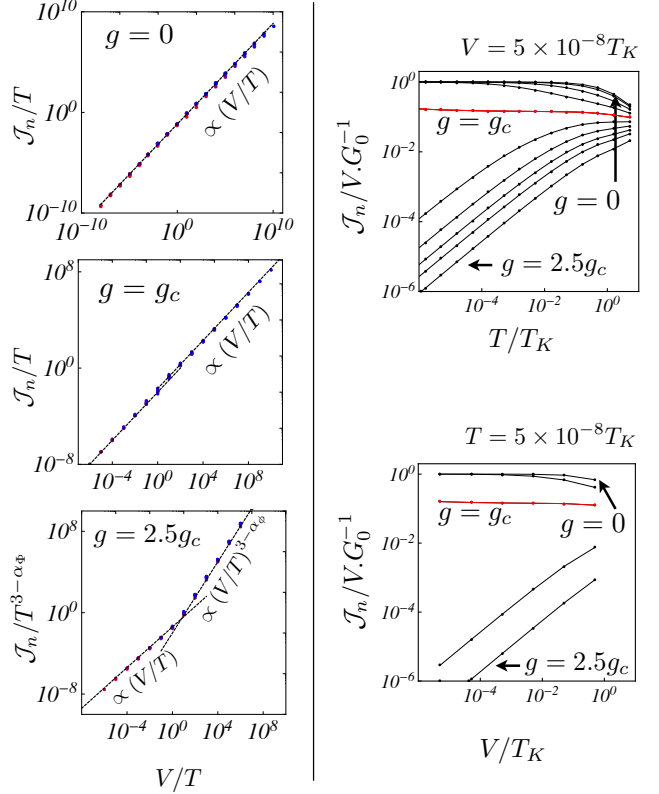


Fig. 3: Left Panel - Scaling of the particle current \mathcal{J}_n as a function of V/T for the different fixed points computed for several temperatures (the color code follows the one of Fig.2). Right Panel - \mathcal{J}_n/V normalized to the conductance of the unitary limit G_0 as a function of temperature (upper panel) and bias voltage (lower panel) for different values of g .

zero. In the limit $\Delta T \rightarrow 0$ and $\bar{T} < T_K$,

$$K = \frac{1}{M} \frac{1}{\bar{T}} \left. \frac{d\mathcal{J}_e}{d\Delta T} \right|_{\Delta T=0}$$

converges to K_0 for $g < g_c$. In the critical regime, K remains finite in the $\Delta T \rightarrow 0$ limit, with $K_c < K_0$. For the LM fixed point K vanishes for $\bar{T} \rightarrow 0$ as $\mathcal{J}_e \propto \Delta T \bar{T}^{3-\alpha_\Phi}$.

Conclusion. – In this work we analyzed the concept of effective temperatures near local quantum criticality focusing on two non-equilibrium setups ((a): $V \neq 0$ and $\Delta T = 0$ and (b): $V = 0$ and $\Delta T \neq 0$) and studied the nonlinear energy and charge currents in the system. The model considered here, the generalized Bose-Fermi Kondo model in a dynamical large N limit, can be solved exactly. We find that for all scaling regimes everywhere in the phase diagram and for all considered non-equilibrium setups, the equilibrium scaling form of the static and most remarkably of the dynamic spin susceptibility can be recovered by utilizing the effective temperature in the equilibrium scaling relations, rather than the temperature of the leads. The effective temperature as a function of the non-equilibrium drive, has been found to be qualitatively different in setups (a) and (b). As local observables can be

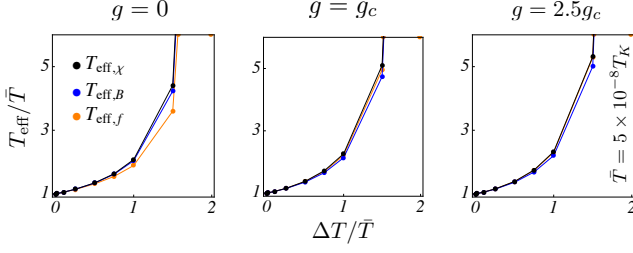


Fig. 4: Effective temperatures for a steady state obtained by imposing $\Delta T \neq 0$ computed in the asymptotic low frequency limit from the FDR of the pseudo-particle propagators and susceptibility.

computed by Wick's theorem, their effective temperature is completely determined by the effective temperatures of the pseudoparticles. Our results therefore suggest that steady-state response near (local) quantum criticality appears thermal albeit an effective temperature. The model considered here is one example of unconventional quantum criticality [17] which has recently been discussed in the context of holographic duals [26]. Very recently, it has been suggested that for quantum critical systems possessing a gravity dual, out-of-equilibrium current noise can appear thermal [15].

It would be very interesting to extend the analysis presented here to other models of steady state quantum criticality and explore the extent to which our findings are generic for quantum critical systems.

This work has been partially supported by NSF and the Robert A. Welch Foundation, Grant No. C-1411.

REFERENCES

- [1] POTHIER H., GUÉRON S., BIRGE N. O., ESTEVE D. and DEVORET M. H., *Phys. Rev. Lett.*, **79** (1997) 3490.
- [2] GROBIS M., RAU I. G., POTOK R. M., SHTRIKMAN H. and GOLDBABER-GORDON D., *Phys. Rev. Lett.*, **100** (2008) 246601.
- [3] ALTIMIRAS C., LE SUEUR H., GENNSER U., CAVANNA A., MAILLY D. and PIERRE F., *Nat Phys*, **6** (2010) 34.
- [4] RIGOL M., DUNJKO V. and OLSHANII M., *Nature*, **452** (2008) 854.
- [5] MITRA A., TAKEI S., KIM Y. B. and MILLIS A. J., *Phys. Rev. Lett.*, **97** (2006) 236808.
- [6] KIRCHNER S. and SI Q., *Phys. Rev. Lett.*, **103** (2009) 206401.
- [7] KHOSRAVI E., UIMONEN A.-M., STAN A., STEFANUCCI G., KURTH S., VAN LEEUWEN R. and GROSS E., *Phys. Rev. B*, **85** (2012) 075103.
- [8] KURTH S., STEFANUCCI G., KHOSRAVI E., VERDOZZI C. and GROSS E. K. U., *Phys. Rev. Lett.*, **104** (2010) 236801.
- [9] HOHENBERG P., *Physica D*, **37** (1989) 109.
- [10] CUGLIANDOLO L. F., KURCHAN J. and PELITI L., *Phys. Rev. E*, **55** (1997) 3898.

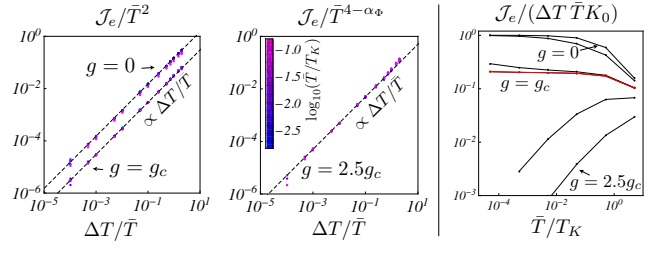


Fig. 5: Left and middle panels - Energy current for the Kondo ($g = 0$), critical ($g = g_c$) and LM ($g = 2.5g_c$) fixed points as a function of $\Delta T/\bar{T}$ computed for several values of \bar{T} (see inset caption). Note the different scaling in the LM case. Right panel - Evolution of $J_e/(\Delta T \bar{T} K_0)$ with \bar{T} at fixed ΔT .

- [11] MITRA A. and MILLIS A., *Phys. Rev. B*, **72** (2005) 121102.
- [12] ARRACHEA L. and CUGLIANDOLO L. F., *EPL*, **70** (2005) 642.
- [13] KIRCHNER S. and SI Q., *Physica Status Solidi (b)*, **247** (2010) 631.
- [14] CASO A., ARRACHEA L. and LOZANO G. S., *Phys. Rev. B*, **83** (2011) 165419.
- [15] SONNER J. and GREEN A. G., *Phys. Rev. Lett.*, **109** (2012) 091601.
- [16] CASO A., ARRACHEA L. and LOZANO G., *Eur. Phys. J. B*, **85** (2012) 266.
- [17] SI Q., RABELLO S., INGERSENT K. and SMITH J. L., *Nature*, **413** (2001) 804.
- [18] ZARÁND G. and DEMLER E., *Phys. Rev. B*, **66** (2002) 024427.
- [19] ZHU L. and SI Q., *Phys. Rev. B*, **66** (2002) 024426.
- [20] ZHU L., KIRCHNER S., SI Q. and GEORGES A., *Phys. Rev. Lett.*, **93** (2004) 267201.
- [21] KIRCHNER S., ZHU L., SI Q. and NATELSON D., *PNAS*, **102** (2005) 18824.
- [22] PARCOLLET O., GEORGES A., KOTLIAR G. and SENGUPTA A., *Phys. Rev. B*, **58** (1998) 3794.
- [23] KAMINSKI A., NAZAROV Y. and GLAZMAN L. I., *Phys. Rev. B*, **62** (2000) 8154.
- [24] KAMENEV A., *Field Theory of Non-Equilibrium Systems* (Cambridge University Press) 2011.
- [25] FOINI L., CUGLIANDOLO L. F. and GAMBASSI A., *Phys. Rev. B*, **84** (2011) 212404.
- [26] IQBAL N., LIU H., MEZEI M. and SI Q., *Phys. Rev. D*, **82** (2010) 045002.